Paredes Paredes, M. C. & Fernández-Getino García, M. J. (2016). Performance of OPS-SAP technique for PAPR reduction in IEEE 802.11p scenarios. *Ad Hoc Networks*, vol. 52, pp. 78–88.

DOI: 10.1016/j.adhoc.2016.07.010

Performance of OPS-SAP Technique for PAPR Reduction in IEEE 802.11p scenarios

Martha Cecilia Paredes Paredes[a,*], M. Julia Fernández-Getino García[b]

[a]*Departamento de Electrónica, Telecomunicaciones y Redes de Información, Escuela Politécnica Nacional, Ladrón de Guevara E11-253, 170517, Quito - Ecuador*
[b]*Department of Signal Theory and Communications, Universidad Carlos III de Madrid, Avda. Universidad 30, 28911, Leganés, Madrid - España*

Abstract

Vehicular Ad Hoc Networks (VANETs) are wireless networks that emerged thanks to the rapid evolution of wireless technologies and the automotive industry. The IEEE 802.11p standard is part of a group of standards related to all layers of protocols for Wireless Access in Vehicular Environment (WAVE) communications, which defines Medium Access Control (MAC) and Physical (PHY) levels. The PHY layer of IEEE 802.11p is essentially based on Orthogonal Frequency Division Multiplexing (OFDM) due to its advantages. However, OFDM signal suffers from high Peak-to-Average Power Ratio (PAPR) at the transmitter side, which causes a significant power efficiency penalty. An efficient peak power reduction technique is Simple Amplitude Predistortion aided by Orthogonal Pilot Sequences (OPS-SAP), which consists in moving a certain outer constellation points of the frequency-domain OFDM symbol. In this paper, we propose the application of this OPS-SAP scheme in the IEEE 802.11p scenario, and, moreover, its evaluation under a complete PHY layer.

Keywords: VANETs, OFDM, PAPR reduction, OPS-SAP

1. Introduction

During the last years, Vehicular Ad- Hoc Networks (VANETs) have gained wide popularity because they allow to disseminate messages to a large set of vehicles traveling along the road. It holds the potential of improving public safety, road traffic management, vehicular traffic coordination and comfort applications [1]. Also, it is important that communications between vehicles are reliable. IEEE 802.11p [2] is part of a set of standards related to the Wireless Access in Vehicular Environment (WAVE) communications. Nevertheless, IEEE 802.11p is limited by the scope of IEEE 802.11 standard, which is strictly for Medium Access Control (MAC) and Physical Layer (PHY).

The PHY of IEEE 802.11p is based on Orthogonal Frequency Division Multiplexing (OFDM) [2], since it has some advantages such as robustness to multipath fading, high bandwidth efficiency, and a simple equalizer structure. However, one of the most serious problems of the OFDM transmitted signal is the high Peak-to-Average Power Ratio (PAPR). When the signal with high peaks goes through the nonlinear zone of a High Power Amplifier (HPA), which is a very sensitive device to signal fluctuations, it leads to in-band distortion, which increases the Bit Error Rate (BER), and out-of-band radiation, which causes adjacent channel interference [3].

The simplest solution to the high PAPR is to backoff the operating point of the HPA, making HPA operates far from the saturation point, but although simple, this approach usually causes a significant power

*Corresponding author at: Departamento de Electrónica, Telecomunicaciones y Redes de Información, Escuela Politécnica Nacional

Email addresses: cecilia.paredes@epn.edu.ec (Martha Cecilia Paredes Paredes), mjulia@tsc.uc3m.es (M. Julia Fernández-Getino García)

efficiency penalty. Many schemes with different features have been proposed in the literature to deal with the large peaks; an overview of these schemes is presented in [4, 5].

The Constellation Extension (CE)-based schemes are one of the most promising techniques since there is no useful data rate decrease, also without Bit Error Rate (BER) degradation, and they do not need the transmission of side information to the receiver. The key of the CE-based methods is that a set of outer constellation points of the frequency-domain transmitted signal are moved toward the outside with an extension factor in such way that the PAPR is decreased. Techniques of this type are Active Constellation Extension (ACE) [6]; CE-based on convex optimization [7, 8]; CE-based on mixed-integer nonlinear programming optmimization, namely GBDCE (Generalized Benders Decomposition for Constellation Extension) [9]; and CE-based on integer-programming, called BBCE (Branch-and-Bound for Constellation Extension) [9]; metric-based CE, named Simple Amplitude Predistortion (SAP) [10]; metric-based Symbol Predistortion [11]; and metric-based schemes embedded with pilot signaling [12, 13].

Most of these schemes, such as ACE [6], CE-based on convex optimization [7, 8], GBDCE and BBCE [9] are formulated as optimization problems, where the computational complexity is very high. To alleviate this load, [10] and [11] propose the calculation of a metric, which defines the set of constellation points that will be expanded, and then, the frequency-domain symbols with the highest metric value are selected to be extended with a predefined scaling factor. This scheme is also known as symbol predistortion technique [10]. Recently, in [12, 13] it has been proposed the combined use of metric-based CE with pilot signaling. This means that SAP technique [10] is aided by Orthogonal Pilot Sequences (OPS) [14] with the purpose of achieving better results than previous schemes. The combination of these proposals leads to three different architectures of implementation, which depends on the position of the algorithms. Two of the schemes are two-step architectures and they are called OPS-SAP and SAP-OPS respectively, and the third one is a simultaneous scheme. Moreover, in [13] it is shown that the OPS-SAP architecture is the most adequate in order to obtain a good trade-off between performance and complexity. However, these schemes were only analyzed in terms of PAPR reduction in a generic scenario, which means that they considered OFDM symbols without the characteristics of any particular standard.

In [15] OPS-SAP performance is evaluated under a specific WAVE environment, this is IEEE 802.11p standard. However, this work is very limited since only a few features of the standard are considered, so that [15] considers only OFDM blocks with IEEE 802.11p specifications. Thus, a complete characterization of the standard is missing. In the literature, almost all existing PAPR reduction techniques assume only a generic OFDM transmission block, in which a successful performance is guaranteed. Nevertheless, the PHY layer of a wireless communications system normally includes other transmission blocks such as encoder, scrambler, interleaver, etc. In this paper we present a complete analysis of this OPS-SAP technique for PAPR reduction under a complete PHY layer of IEEE 802.11p standard and we extend our simulations to different modulations and coding rates. It is stated through simulation results that OPS-SAP technique is a good choice to efficiently reduce PAPR in an IEEE 802.11p scenario. The remainder of this paper is organized as follows. Section 2 introduces the OFDM-PHY model for the IEEE 802.11p standard, PAPR definition and PAPR performance evaluation way. Section 3 provides a review of OPS-SAP technique. In Section 4, simulation results are presented. Finally, the conclusions are drawn in Section 5.

2. OFDM-PHY layer in IEEE 802.11p

PHY layer of a wireless communications system covers all steps to carry the binary data to the wireless channel. This section provides a revision of the PHY entity for OFDM system in IEEE 802.11p standard. The OFDM system in IEEE 802.11p provides a half-clocked operation using 10 MHz channel spacing with different data communication capabilities. The PHY of the standard IEEE 802.11p consists of Physical Medium Dependent (PMD) sublayer and Physical Layer Convergence Protocol (PLCP) sublayer.

On one hand, the PMD sublayer specifies signal build-up parameters, such us modulation, channel coding and how to convert signal into analog form. IEEE 802.11p PMD sublayer uses OFDM Modulation. On the other hand, the PLCP sublayer carries out a convergence procedure, in order to deal with differences among various PHY, and ensures that the MAC layer receives packets of common format, independently of particular PMD sublayer.

Convergence procedure performed by PLCP sublayer converts the actual data frame, called PLCP Service Data Unit (PSDU) into PLCP Protocol Data Unit (PPDU). In terms of this convergence, the PSDU is appended with preamble and header.The PLCP preamble is shown in Fig. 1, which consists of ten $1.6\mu s$-length repetitions of a short training sequence $(t_1, \cdots, t_{10})$ that are used for packet detection and synchronization. Then, two $6.4\mu s$-length repetitions of a long training sequences (T_1, T_2), that are used to estimate the channel. A guard interval $(GI2)$ of $3.2\mu s$ is between the training sequences. Then,the SIGNAL field contains information about data rate and length of packet, followed by the packet data payload. All symbols are of length $8\mu s$, which include a guard interval (GI) of $1.6\mu s$ between data symbols.

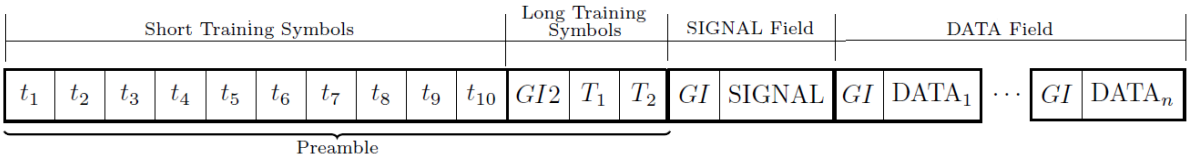

Figure 1: IEEE 802.11p PHY packet preamble structure

The PSDU is encoded and modulated. The encoding process is composed of scrambling, encoding, interleaving and possibly puncturing, in order to achieve higher data rates. These transmission blocks are sketched in the diagram of Fig. 2.

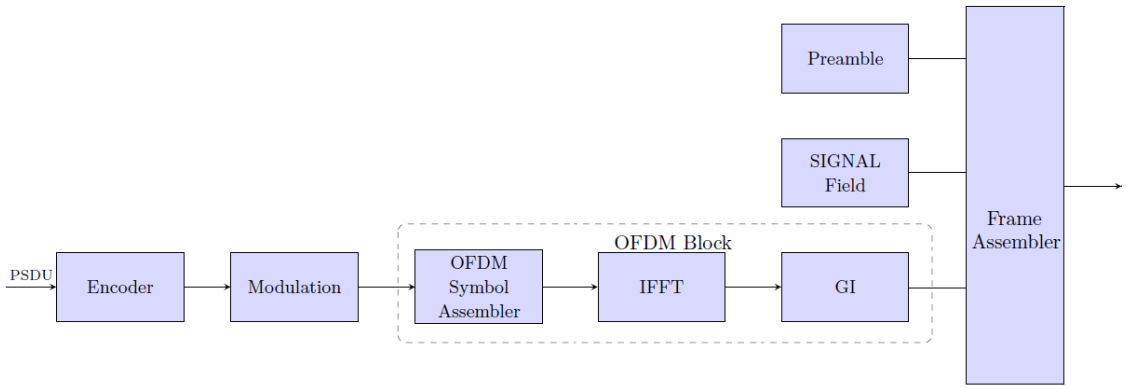

Figure 2: Block diagram of the transmitter in IEEE 802.11p.

The bits of the PSDU frame are scrambled with the aim of randomizing the data pattern, which may contain long strings of ones or zeros. The IEEE 802.11p scrambler uses the generator polynomial $\mathcal{S}(x)$, as follows

$$\mathcal{S}(x) = x^7 + x^4 + 1 \tag{1}$$

Then, the scrambled data is passed to a convolutional encoder, which introduces, in a controlled manner, some redundancy into the bit stream. This redundancy is used for error correcting coding which allows the receiver to combat the detrimental effects of the channel. Convolutional coding makes use of linear shift registers. The connection of the shift register taps to the modulo-2 adders is represented by generator polynomials $g_0 = 133_8 = [01011011]_2$ and $g_1 = 171_8 = [01111001]_2$ of rate 1/2. Higher rates (2/3 and 3/4) are derived from it by employing puncturing [2]. Puncturing is a procedure for omitting some of the encoded bits in order to reduce the number of transmitted bits and then increasing the coding rates [2]. At the receiver side, decoding by the Viterbi algorithm is recommended [2].

Next, all encoded bits shall be interleaved by an interleaving block with a block size corresponding to the number of bits in a single OFDM symbol, N_{CBPS}. The interleaving scheme is used to cope with the correlated channel noise such as burst errors or fading. For IEEE 802.11p PHY, the interleaving scheme is

Table 1: IEEE 802.11p modulation-dependent parameters

Coding Rates (R)	***Modulation***	***Coded Bits Per Subcarrier*** (N_{BPSC})	***Coded Bits Per OFDM Symbol*** (N_{CBPS})	***Data Bits Per OFDM Symbol*** (N_{DBPS})	***Data Rate*** (Mb/s)
1/2	BPSK	1	48	24	3
3/4	BPSK	1	48	36	4.5
1/2	QPSK	2	96	48	6
3/4	QPSK	2	96	72	9
1/2	16-QAM	4	192	96	12
3/4	16-QAM	4	192	144	18
2/3	64-QAM	6	288	192	24
3/4	64-QAM	6	288	216	27

defined by two-step permutations. The first permutation ensures that the adjacent coded bits are modulated onto nonadjacent subcarriers. Next, the second permutation ensures that the adjacent coded bits are mapped alternatively onto less and more significant bits of the constellation. The first permutation is defined by the next rule

$$i = (N_{CBPS}/16) + \text{Floor}\,(k/16)\,, \qquad k = 0, \ldots, N_{CBPS} - 1 \tag{2}$$

where Floor $(\cdot)$ denotes the largest integer not exceeding the parameter.

The second permutation is given by the next rule

$$i = s \times \text{Floor}\,(i + N_{CBPS} - \text{Floor}\,(16 \times i/N_{CBPS}))\,\text{s}, \qquad i = 0, \ldots, N_{CBPS} - 1 \tag{3}$$

where the value of s is determined by the number of coded bits per subcarrier (N_{BPSC}) according to

$$s = \max\,(N_{BPSC}/2, 1) \tag{4}$$

where max $(\cdot)$ function yields the maximum value of the input vector.

In this standard, the modulation type defines four constellations: BPSK (Binary Phase Shift Keying), QPSK (Quadrature Phase Shift Keying), 16-QAM (Quadrature Amplitude Modulation) and 64-QAM Therefore, the encoded and interleaved binary serial input data are divided into groups of N_{BPSC} bits and converted into complex numbers representing the constellation points. The conversion is performed according to Gray-coded constellation mapping.

For transmission, an OFDM symbol is implemented using 64-points Inverse Fast Fourier Transform (IFFT). From those 64 available subcarriers, $N_{SD} = 48$ are used for data transportation, $N_{SP} = 4$ are pilot subcarriers, another 11 subcarriers are null for separating the subbands and DC subcarrier is also not used [16]. More details about OFDM signal are analyzed in the next subsection.

In combination with different coding rates, this leads to a nominal data rate of 3 to 27 Mb/s, as summarized in Table 1. IEEE 802.11p uses the half clocked mode with 10MHz bandwidth, in order to make signal more robust against fading. This fact leads to a data rate reduction compared to IEEE 802.11a standard.

The receiver basically performs the reverse operation. In addition, it has to manage the Automatic Gain Control (AGC), the time and frequency synchronization, the equalization and channel estimation [17]. To support this functions, training sequences are provides in the preamble of each packet.

2.1. OFDM Modulation

OFDM is a multicarrier transmission technique, which divides the available bandwidth W into N parallel subcarriers with equal bandwidth W/N. Each subcarrier corresponds to a frequency f_k where $k = \{0, \cdots, N-1\}$. Then, each OFDM symbol, in frequency-domain, $\mathbf{X} = \{X(k)\}_{k=0}^{N-1}$ is a block of N

complex symbols (using an specific constellation: BPSK, QPSK, 16-QAM, etc.) over kth subcarrier. The time-domain OFDM signal is generated by multiplexing these N independent signals, which can be efficiently implemented by an Inverse Discrete Fourier Transform (IDFT) operation. Then the time-domain signal $\mathbf{x} = \{x[n]\}_{n=0}^{N-1}$ is given by:

$$x[n] = \frac{1}{\sqrt{N}} \sum_{k=0}^{N-1} X(k) e^{j\frac{2\pi}{N}kn}, \quad 0 \leq n < N-1 \tag{5}$$

where k and n are the frequency and time indices respectively.

After the transformation in time-domain is completed, each OFDM symbol is preceded by a periodic extension of itself, thus forming the Cyclic Prefix (CP) in order to prevent InterSymbol Interference (ISI) caused by multipath propagation and InterCarrier Interference (ICI). Duration of the cyclic prefix in this standard is given by

$$T_{CP} = \frac{T_{FFT}}{4} \tag{6}$$

where $T_{FFT} = 6.4\mu s$ is the IFFT/FFT period in IEEE 802.11p standard. Hence, the CP is just a copy of the last 16 samples of each OFDM symbol.

2.2. PAPR Problem

The frequency-domain signal $\mathbf{X} = \{X(k)\}_{k=0}^{N-1}$ are independent, identically distributed (i.i.d.) random variables and, based on the central limit theorem, most samples in time-domain will have low values but a small percentage of them will take very large magnitudes. This results in the well-known PAPR problem of OFDM systems. In general, the PAPR (denoted as χ) of the time-domain signal $x[n]$ is mathematically defined as the ratio between the maximum instantaneous power and its average power [18], that is:

$$\begin{aligned} \chi &= PAPR\{x[n]\} \\ &= \frac{\max\left(|x[n]|^2\right)}{E\left\{|x[n]|^2\right\}}, \quad 0 \leq n < N-1 \end{aligned} \tag{7}$$

where $E\{\cdot\}$ denotes expected value and $|\cdot|$ is the modulo operation.

The performance of PAPR reduction schemes is commonly evaluated by three main parameters: Complementary Cumulative Distribution Function (CCDF), spectral spreading and BER. Also, Packet Error Rate (PER) is very illustrative to evaluate network performance.

2.2.1. Complementary Cumulative Distribution Function (CCDF)

Complementary Cumulative Distribution Function (CCDF) is often used to evaluate PAPR reduction techniques. The CCDF determines the probability that the PAPR exceeds a certain threshold χ_0. Thus the CCDF can be written as [19].

$$CCDF(\chi) = Prob(\chi > \chi_0) = 1 - 1(1 - e^{-\chi_0^2})^N \tag{8}$$

2.2.2. Spectral Spreading

An HPA is a particularly sensitive device to the signal fluctuations. In order to analyze the amount of distortions introduced by the HPA, it is recommended to evaluate the behavior of a PAPR reduction scheme at the output of an HPA by observing the Power Spectral Density (PSD).

In general, modeling an HPA is complicated, but a common approach is to model it as memoryless nonlinearities with frequency-nonselective response [5]. If the input of the HPA is given by

$$x[n] = |x[n]|e^{j\theta[n]} \tag{9}$$

where $|x[n]|$ and $\theta[n]$ are the amplitude and the phase of the input signal, respectively, then the output is given by

$$y[n] = G\left(|x[n]|\right)\, e^{\{j\theta[n]+\Phi[|x[n]|]\}}, \tag{10}$$

where $G(\cdot)$ and $\Phi(\cdot)$ are the AM/AM and AM/PM conversion functions, respectively. $G(\cdot)$ shows the effect of nonlinearities on the amplitude $|x[n]|$, and $\Phi(\cdot)$ accounts for the effect of nonlinearity on the phase $\theta[n]$.

A common configuration used in IEEE 802.11p standard is a Solid State Power Amplifier (SSPA) [20], which can be modelled according to the modified Rapp's SSPA model [21], where the amplitude/phase (AM/PM) and amplitude/amplitude (AM/AM) characteristics are expressed as:

$$G\left(|x[n]|\right) = \frac{|x[n]|}{\left(1+\left(|x[n]|/A_{sat}\right)^{2p}\right)^{\frac{1}{2p}}} \tag{11}$$

$$\Phi\left(|x[n]|\right) \approx 0 \tag{12}$$

being p a parameter that controls the smoothness of the characteristic (the smaller p, the smoother the characteristic) and A_{sat} is the saturation level of SSPA. Note that the AM/PM of SSPA is zero.[1]

2.2.3. Bit Error Rate (BER)

The performance of a modulation technique can be quantified in terms of the required Signal-to-Noise Ratio (SNR) to achieve a specific BER. Although the main focus of PAPR reduction techniques is to reduce the peaks, some PAPR reductions techniques usually achieve this aim at the expense of increasing the BER. Therefore, its evaluation is of great interest.

2.2.4. Packet Error Rate (PER)

Packet Error Rate (PER) is an important Quality of Service (QoS) parameter for wireless networks. In IEEE 802.11p standard, a packet is received correctly if it passes the Cyclic Redundancy Check (CRC) procedure (all bits are correct). These terms are closely linked, i.e. with a given packet length and BER, PER can be calculated using the following formula [22]

$$\mathrm{PER} = 1 - (1 - \mathrm{BER})^{l} \tag{13}$$

where l denotes packet length.

3. OPS-SAP Technique for PAPR Reduction

Here, we describe the OPS-SAP technique for PAPR reduction , which is a two-step algorithm. OPS-SAP consists in a metric-based CE scheme, named SAP, aided by OPS scheme [12].

This proposal follows the steps shown in the diagram of Fig. 3, in which the main building blocks are SAP and OPS stages. The first step consists in inserting the pilot sequence of the available set such that the pilot sequence that provides the lowest PAPR is chosen. And, the second step carries out the extension of the frequency-domain symbols (either pilots or data) by a metric calculation in order to decide which symbols will be extended. Next, we provide a more detailed explanation of the OPS-SAP scheme.

3.1. OPS stage

In an OFDM symbol with N subcarriers, a subset Υ of subcarriers will carry pilot symbols and thus, the input data sequence $X(k)$ is given by:

$$X\left(k\right) = \begin{cases} D(k), & k \notin \Upsilon \\ P(k), & k \in \Upsilon \end{cases} \tag{14}$$

[1]The effect of the AM/PM conversion is not exactly zero, but it is very small and thus it is not considered in the SSPA model.In this case, the Rapp's SSPA model introduces only AM/AM distortion.

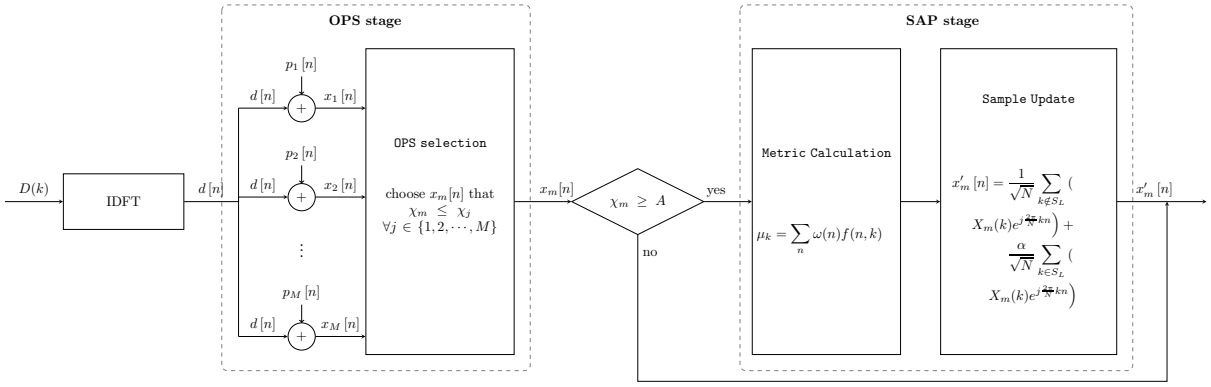

Figure 3: Block diagram of OPS-SAP scheme.

where $D(k)$ and $P(k)$ are data and pilot symbols, respectively.

The transmitted time-domain signal $x[n] = d[n] + p[n]$ can be also separated into two parts, as:

$$x\,[n] = \begin{cases} d\,[n] & = \frac{1}{\sqrt{N}} \sum_{k \notin \Upsilon} D(k) e^{j\frac{2\pi}{N}kn} \\ p\,[n] & = \frac{1}{\sqrt{N}} \sum_{k \in \Upsilon} P(k) e^{j\frac{2\pi}{N}kn} \end{cases} \tag{15}$$

where $d\,[n]$ and $p\,[n]$ refer to the time-domain data and pilot signals, respectively. They are obtained by IFFT operation given in (5).

OPS technique [14] proposes the use of a predetermined set of M orthogonal pilot sequences of length N_{SP} ($M \leq N_{SP}$). In fact, N_{SP} is the cardinality of the set Υ. The N_{SP} pilot symbols of each OFDM symbol can be collected in an $N-$length sequence denoted as $\mathbf{P}$ where, the kth element of this sequence is given by:

$$[\mathbf{P}]_k = \begin{cases} P(k), & k \in \Upsilon \\ 0 & k \notin \Upsilon \end{cases} \tag{16}$$

As stated before, a set of M pilot sequences is available so the alphabet is $\mathbf{P} \in \{\mathbf{P}_1, \mathbf{P}_2, \cdots, \mathbf{P}_M\}$. Each pilot sequence of this finite set $\mathbf{P}_m$, $m = \{1, \cdots, M\}$ contains the frequency-domain pilot symbols at pilot positions while zeros are inserted in the remaining ones. These pilot sequences are orthogonal so then the orthogonality condition is fulfilled:

$$\langle \mathbf{P}_m, \mathbf{P}_\ell \rangle = 0 \quad m \neq \ell \quad m, \ell = \{1, \cdots, M\} \tag{17}$$

where $\langle \cdot, \cdot \rangle$ denotes the inner product.

In particular, if the well-known Walsh-Hadamard sequences are employed where $P(k) \in \{1, -1\}$, then $\langle \mathbf{P}_m, \mathbf{P}_\ell \rangle = N_{SP}\delta[m - \ell]$, $m, \ell = \{1, \cdots, M\}$, where $\delta[\cdot]$ denotes the Kronecker delta function.

When implementing OPS, we can make use of time-domain processing to reduce complexity [12] unlike OPS proposed in [14]. In this case, the orthogonal pilot sequences are previously generated in time-domain via IDFT-operation. They are stored and later used, thus avoiding $(M-1)$ IDFT operations.

In OFDM symbol of IEEE 802.11p there are $N_{SP} = 4$ pilot symbols and the subset Υ is $\{-27, -7, 7, 27\}$. Also, a set of $M = 4$ sequences is considered to carry out OPS stage.

3.2. SAP stage

The key of this stage is to play intelligently with the outer constellation points of the frequency-domain signal $X(k)$ (either data or pilots symbols). This idea is clearly illustrated in Fig. 4, where the 16-QAM constellation points are classified into three groups: inner points, boundary points, and corner points. The inner points can not be moved in order to not affecting the minimum distance; the boundary points are moved in the arrow direction, this is, either the real or the imaginary part; and the corner points are moved within their external quadrant. In Fig. 4 the shaded region represents the allowed extension region.

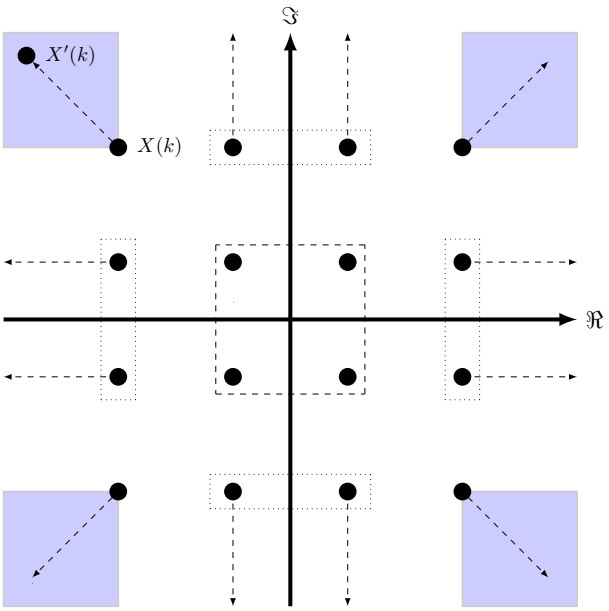

Figure 4: Allowed regions for 16-QAM modulation

In order to determine the set of indices of $X(k)$ that are moved or predistorted, SAP employs a metric calculation, defined mathematically in (18). This metric measures the contribution of frequency-domain symbols with large peaks to the time-domain samples.

$$\mu_k = \sum_n \omega(n) f(n,k) \tag{18}$$

where, $f(n,k) = -\cos(\varphi_{nk})$ is a function which measures the phase angle (φ_{nk}) between $x[n]$ and $X(k)$, $\omega(n) = |x[n]|^p$ is a weighting function which gives more weight to the time-domain samples with large magnitudes, and p is a selected parameter [10]. Then, the metric is computed for all input symbol and the $L = |S_L|$ frequency-domain symbols, that belong to the set of indices of frequency-domain symbols S_L, with the greatest positive metric values are selected and extended with a constant scaling factor $\alpha > 1$. This is,

$$X'(k) = \begin{cases} \alpha X(k) & k \in S_L \\ X(k) & k \notin S_L \end{cases} \tag{19}$$

where $X'(k)$ represents the extended frequency-domain signal. Then, its corresponding time-domain symbol will be updated.

In [10], the size of the subset L and the value of the constant scaling factor α are chosen from a group of values suggested empirically, and these are: $L = 10$ with $\alpha = 2$, $L = 26$ with $\alpha = 1.55$ and $L = 40$ with $\alpha = 1.3$.

The benefits of this architecture (OPS-SAP) are that, first, it outperforms previous methods (SAP, OPS) in terms of PAPR reduction. Also, from an efficiency point of view, we can carry out the amplitude predistortion in this scheme with less energy per complex symbol than in SAP, if we adequately use the smart pilots to get an energy efficient system.

The drawbacks of this joint procedure are: (1) it is only intended for coherent systems with pilot symbols, and (2) it implies a slight increase in complexity, compared to SAP alone, since low-complex OPS must be carried out. However, this additional computational burden is negligible since only a search over M sequences is performed.

Table 2: PHY parameters of IEEE 802.11p standard

Parameter	***Value***
Bit Rate (Mb/s)	3,4.5,6,9,12,18,24,27
Modulation mode	BPSK, QPSK, 16-QAM, 64-QAM
Code Rate (R)	$1/2, 2/3, 3/4$
Number of data subcarriers (N_{SD})	48
Number of pilot subcarriers (N_{SP})	4
Number of total Subcarriers (N_{ST})	52 ($N_{SD} + N_{SP}$)
Subcarrier frequency spacing (Δ_F)	0.15625 MHz
FFT period (T_{FFT})	$6.4\mu s\,(1/\Delta_F)$
Preamble period ($T_{PREAMBLE}$)	$32\mu s$
Guard duration (T_{GI})	$1.6\mu s\,(T_{FFT}/4)$
Symbol duration (T_{SYM})	$8\mu s\,(T_{FFT} + T_{GI})$
PSDU length (l)	10
Average Power	1.4720 dB

4. Simulation Results

In this section, we present the evaluation of the OPS-SAP technique for PAPR reduction under a complete OFDM-PHY layer in the IEEE 802.11p standard.

The simulation scenario consists in computer simulations, that are carried out by averaging 10^4 randomly generated PSDU frames. The PSDU are generated by random binary sequences. The number of generated random bits depends on coding rates, the modulation scheme, as well on the number of transmitted OFDM data symbols.

The PSDU frames are encoded and then modulated (see Fig. 2). The encoding process is composed of scrambling, encoding, interleaving and puncturing, in order to achieve different data rates (see the relation between these parameters in Table 1).

The OPS-SAP PAPR reduction scheme is evaluated in terms of CCDF, Spectral Spreading, BER and PER. We also compare OPS-SAP with SAP and OPS schemes. The parameters of OPS-SAP proposal are $\alpha = 1.55$ and $L = 26$ for the SAP stage and $N_{SP} = 4$, $M = N_{SP}$ for OPS stage; OPS and SAP alone are considered with the same parameters. We also provide several results with different parameters of PHY layer. In Table 2, we summarized some parameters of IEEE 802.11p PHY, which are used in the simulations.

In order to show the improvement in performance of OPS-SAP scheme, in terms of CCDF, Fig. 5 presents the CCDF of PAPR when OPS-SAP scheme is applied in IEEE 802.11p with different configurations on PHY layer. We considered OFDM systems with all possible combinations of modulation and coding rate (see Table 1) in order to achieves different bit rates. We compared OPS-SAP technique with respect to OFDM signal without any PAPR reduction technique (labelled as "Original") with the same modulation and coding rate. In this figure, the dashed line curves represent the "Original" performance and the solid line curves shows the OPS-SAP performance. It is observed that OPS-SAP for IEEE 802.11p with BPSK and QPSK modulation (3, 4.5, 6 and 9 Mb/s) present better results than IEEE 802.11p with 16-QAM and 64-QAM modulations (12, 18, 24 and 27 Mb/s) since the extended symbols in high-order modulations do not necessarily correspond to those symbols with the highest metric value because the inner points of the constellation are not considered in the predistortion process (see Fig. 4). For example, one of the best results is obtained for IEEE 802.11p with 6 Mb/s when OPS-SAP algorithm is applied, which represents a reduction of approximately 2.7 dB at a probability of 10^{-3} with respect to the "Original" with the same data rate. And, also, there is a reduction of approximately 1.6 dB and 1 dB at a probability of 10^{-3} for IEEE 802.11p with 12 Mb/s and 18 Mb/s, respectively.

With the aim of presenting the improvement in performance of the OPS-SAP scheme compared to other proposals (SAP and OPS). Fig. 6 shows the performance of the OPS-SAP scheme for one of the sets of

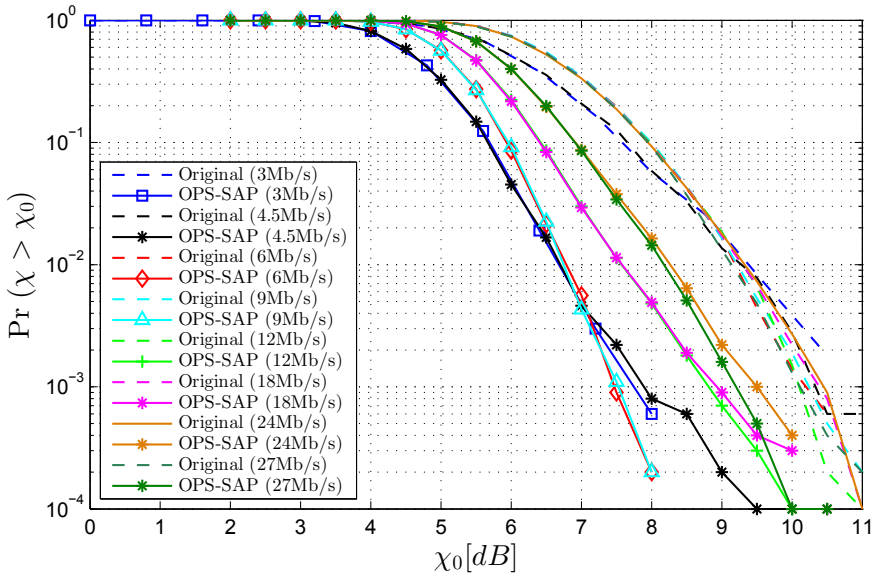

Figure 5: Comparison of CCDF of OPS-SAP for PAPR reduction of IEEE 802.11p with different bit rates.

parameters that provides better results in performance (see Fig. 5), *i.e.* we choose IEEE 802.11p for 6 Mb/s. In this figure, the blue line curve represents the "Original" performance. The marked solid line curves correspond to OPS and SAP algorithms, and the black solid curve depicts the OPS-SAP technique. The OPS-SAP algorithm represents a reduction of approximately 3 dB, 2 dB and 1.2 dB at a probability of 10^{-3} with respect to the conventional OFDM signal, OPS and SAP schemes, respectively.

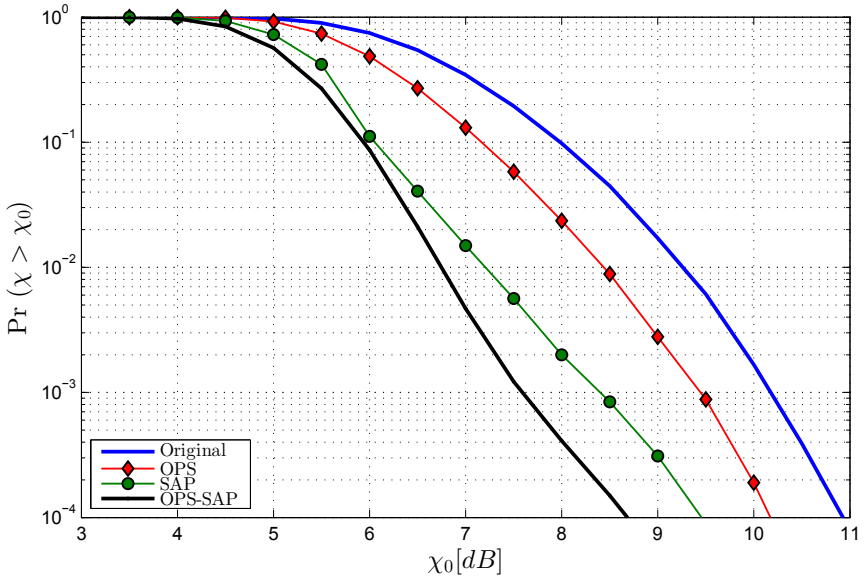

Figure 6: CCDF of OPS-SAP technique for PAPR reduction in an OFDM system compared to OPS and SAP techniques for IEEE 802.11p with 6 Mb/s.

We also observed the PSD (Power Spectral Density) at the output of a nonlinear HPA. A common

configuration used in IEEE 802.11p standard is a Solid State Power Amplifier (SSPA) [20]. Fig. 7 shows the PSD at the output of the SSPA for the "Original" and OPS-SAP signal, with different bit rates, and oversampling factor $J = 3$. The SSPA operates at a value of Input Back-Off IBO = 6 dB and $p = 2$. In this figure, the dashed line curves represent the "Original" (conventional OFDM signal without any PAPR reduction technique) performance and the solid line curves shows the OPS-SAP performance. The OPS-SAP scheme achieves a reduction of this out-of-band radiation with respect to the "Original" signal. For instance, OPS-SAP technique achieves a reduction of the out-of-band radiation of about 2 dB for each PHY configuration.

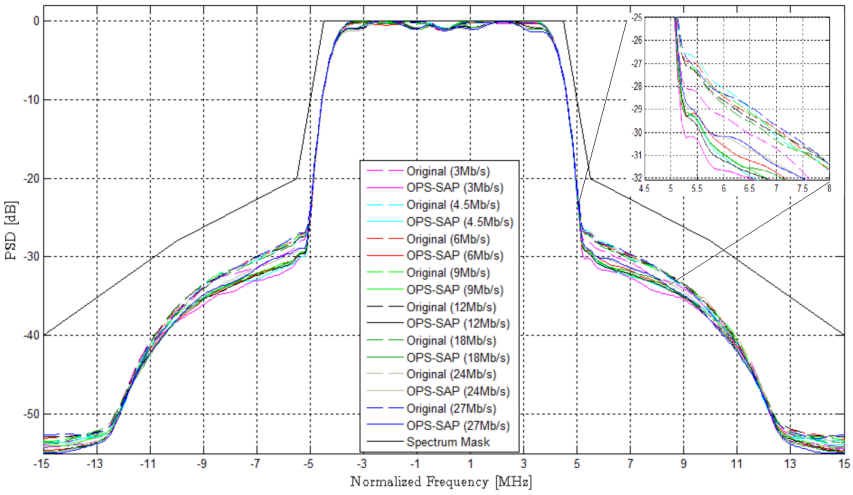

Figure 7: PSD at the output of the SSPA, IBO = 6 dB, OFDM signal with OPS-SAP for different bit rates.

Additionally, OPS-SAP technique is evaluated to confirm that no BER degradation occurs when we transmit using a nonlinear SSPA with IBO = 6 dB and $p = 2$. We contemplate the use of an Additive White Gaussian Noise (AWGN) channel. The Signal-to-Noise Ratio (SNR) is defined as the ratio between the average signal power and the average noise power. As expected, in Fig. 8 a better performance for each PHY configuration is observed when OPS-SAP technique is applied with respect to its corresponding "Original" curve. This is due to two factors: i) the constellation expansion performed by OPS-SAP does not affect the minimum distance of the constellation; and ii) the constellation expansion increases the energy of some constellations points, which leads to a lower BER. For instance, the gain in SNR of the OPS-SAP (for each PHY configuration) scheme is approximately 0.5 dB with respect to the "Original" signal to meet BER= 10^{-3}.

Finally, we discuss the PER performance when OPS-SAP scheme is applied in IEEE 802.11p standard. The PER in calculated after demodulation and decoding processes.

Fig. 9 shows PER against SNR for OFDM-PHY with different bit rates. The packet length is $l = 10$. In this figure, the dashed line curves represent the "Original" signal and the solid line curves shows the OPS-SAP performance. It is seen that there is not degradation in PER when OPS-SAP is applied. In fact, there is an improvement in PER when OPS-SAP is carried out. To cite an instance, the PER gain is approximately 0.5 dB with respect to the "Original" to meet BER= 10^{-3}.

We also present PER results vs packet length (l) in Fig. 10 for different PHY configurations. This figure shows that in general the PER is lower for short packets than for long packets, since for the same BER value, the FEC (Forward Error Correction) scheme is more effective with short packets. Moreover, it is observed that when OPS-SAP scheme is applied the PER presents a gain with respect the "Original" case due to the constellation extension process in frequency-domain signal when OPS-SAP scheme is applied in order to reduce the PAPR.

The results of Figures 8, 9 and 10 , confirm that CE-based techniques, including OPS-SAP scheme, are

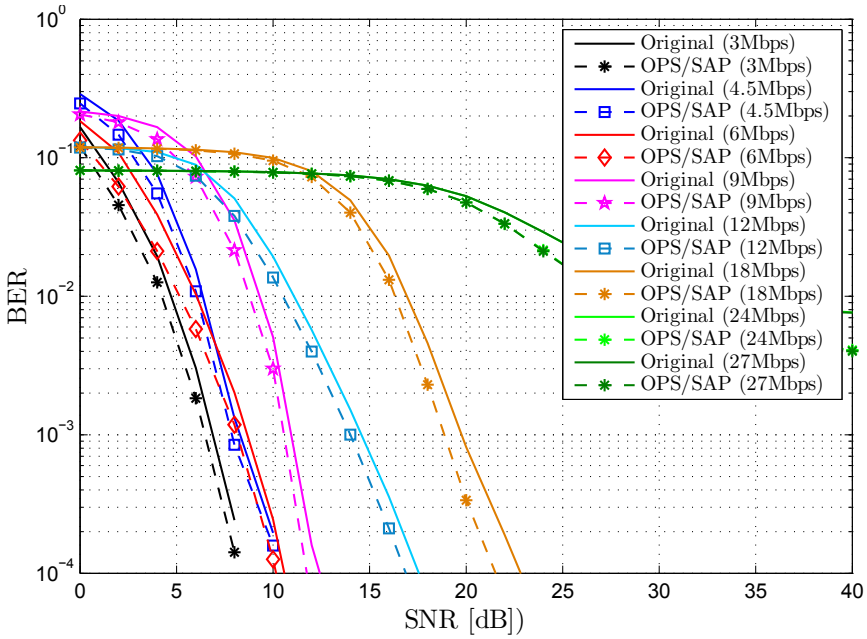

Figure 8: BER performance for OFDM compliant with IEEE 802.11p standard with different modulations and coding rates over an AWGN channel.

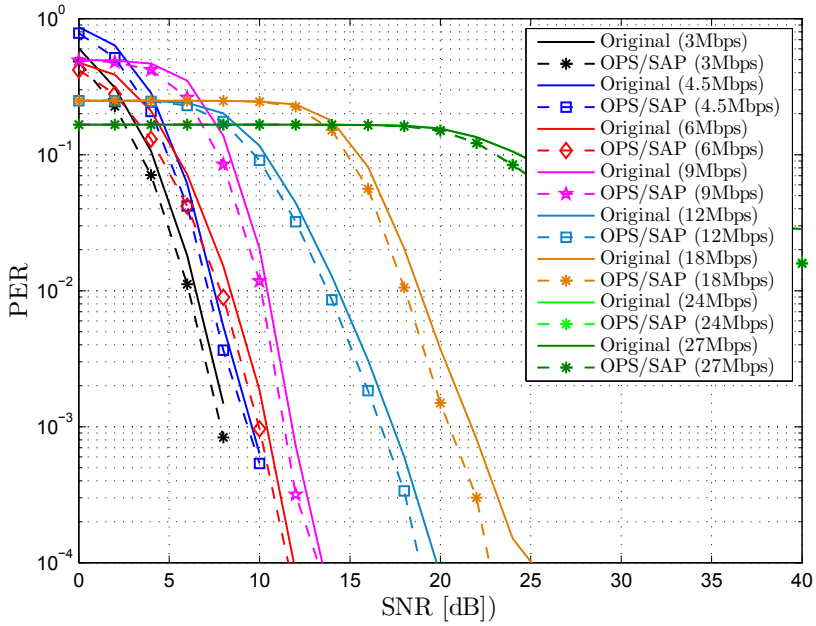

Figure 9: PER performance for OFDM compliant with IEEE 802.11p standard with different bit rates for packet length $l = 10$.

distortionless schemes and, as a consequence, no BER or PER degradation is experienced. We also observe that OPS-SAP presents better results for low-order modulations due to the fact that the predistorted symbols

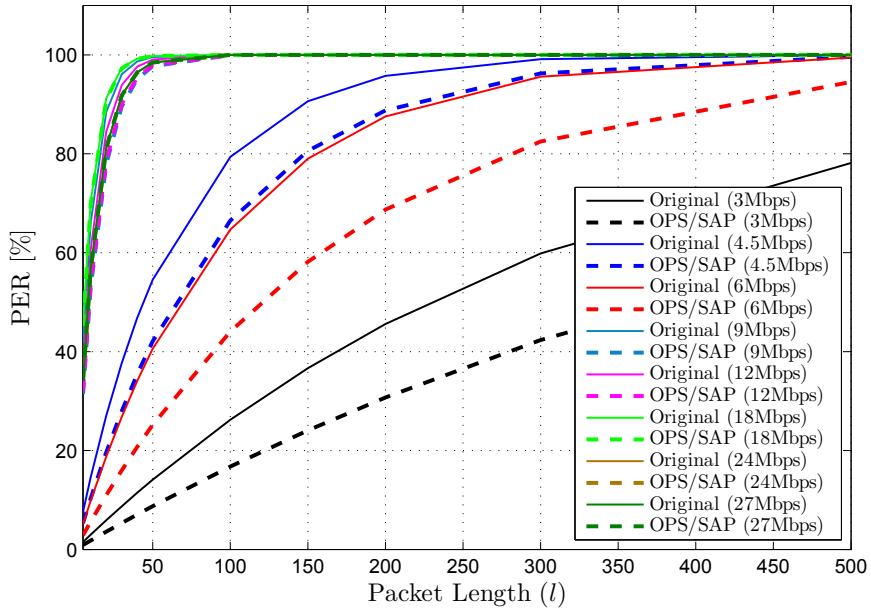

Figure 10: PER performance vs. packet length (l) for OFDM compliant with IEEE 802.11p standard with different bit rates for SNR=8 dB.

do not necessarily correspond to those symbols with the highest metric value because the inner points of the constellation are not considered in the predistortion process.

Regarding the comparison of OPS-SAP scheme with CE techniques based on optimization algorithms, they have not been taken into account in the simulation scenario since these schemes are too complex. However, in [9] some results show a performance comparison between different CE techniques based on convex and non-linear optimization processes.

5. Conclusions

In this work, we evaluate OPS-SAP technique for PAPR reduction under a complete OFDM-PHY layer for Vehicular Ad Hoc Networks (VANETs) context. OPS-SAP is a Constellation Extension (CE)-based scheme, in which certain outer constellation points of the complex transmitted signal are moved outward with a constant extension factor in such way that the signal's peaks in the time-domain are decreased. However, this symbol extension is carried out energy efficiently in OPS-SAP, unlike previous works, by the joint use of OPS. This provides successful results for IEEE 802.11p standard with a simple yet flexible technique. Moreover, a complete performance evaluation, considering different modulations and coding rates, is carried out in order to confirm the suitability of OPS-SAP in WAVE scenarios.

6. Acknowledgments

This work has been supported by the Spanish National Projects GRE3N-SYST (TEC2011-29006-C03-03) and ELISA (TEC2014-59255-C3-3-R) and also by Escuela Politécnica Nacional (Ecuador) by PII-DETRI-01-2016 Project.

References

[1] S. Al-Sultan, M. M. Al-Doori, A. H. Al-Bayatti, H. Zedan, A comprehensive survey on vehicular ad hoc network, Journal of network and computer applications 37 (2014) 380–392.

[2] IEEE, IEEE Standard for Information technology– Local and metropolitan area networks– Specific requirements– Part 11: Wireless LAN Medium Access Control (MAC) and Physical Layer (PHY) Specifications Amendment 6: Wireless Access in Vehicular Environments, IEEE Std 802.11p-2010 (Amendment to IEEE Std 802.11-2007 as amended by IEEE Std 802.11k-2008, IEEE Std 802.11r-2008, IEEE Std 802.11y-2008, IEEE Std 802.11n-2009, and IEEE Std 802.11w-2009) (2010) 1–51doi:10.1109/IEEESTD.2010.5514475.

[3] F. Danilo-Lemoine, D. Falconer, C.-T. Lam, M. Sabbaghian, K. Wesolowski, Power backoff reduction techniques for generalized Multicarrier waveforms, EURASIP Journal on Wireless Communications and Networking 2008 (1) (2008) 437–801. doi:10.1155/2008/437801.
URL http://jwcn.eurasipjournals.com/content/2008/1/437801

[4] T. Jiang, Y. Wu, An overview: Peak-to-Average Power Ratio Reduction Techniques for OFDM signals, IEEE Transactions on Broadcasting 54 (2) (2008) 257–268. doi:10.1109/TBC.2008.915770.

[5] Y. Rahmatallah, S. Mohan, Peak-To-Average Power Ratio Reduction in OFDM Systems: A Survey And Taxonomy, IEEE Communications Surveys Tutorials 15 (4) (2013) 1567–1592. doi:10.1109/SURV.2013.021313.00164.

[6] B. S. Krongold, D. L. Jones, PAR reduction in OFDM via active constellation extension, IEEE Transactions on Broadcasting 49 (3) (2003) 258–268. doi:10.1109/TBC.2003.817088.

[7] C. Wang, S. H. Leung, Par reduction in OFDM through convex programming, in: IEEE International Conference on Acoustics, Speech and Signal Processing (ICASSP) 2008, 2008, pp. 3597–3600. doi:10.1109/ICASSP.2008.4518430.

[8] Z. Yu, R. Baxley, G. Zhou, Generalized interior-point method for constrained peak power minimization of OFDM signals, in: IEEE International Conference on Acoustics, Speech and Signal Processing (ICASSP), 2011, 2011, pp. 3572–3575. doi:10.1109/ICASSP.2011.5946250.

[9] M. C. Paredes Paredes, M. J. Fernández-Getino García, PAPR reduction via Constellation Extension in OFDM systems using Generalized Benders Decomposition and Branch and Bound techniques, IEEE Transactions on Vehicular Technology PP (99) (2015) 1–1. doi:10.1109/TVT.2015.2450178.

[10] S. Sezginer, H. Sari, OFDM peak power reduction with simple amplitude predistortion, IEEE Communications Letters 10 (2) (2006) 65–67. doi:10.1109/LCOMM.2006.02015.

[11] S. Sezginer, H. Sari, Metric-Based symbol predistortion techniques for peak power reduction in OFDM systems, IEEE Transactions on Wireless Communications 6 (7) (2007) 2622–2629. doi:10.1109/TWC.2007.05955.

[12] M. C. Paredes Paredes, M. J. Fernández-Getino García, Energy efficient peak power reduction in OFDM with amplitude predistortion aided by orthogonal pilots, IEEE Transactions on Consumer Electronics 59 (1) (2013) 45–53. doi:10.1109/TCE.2013.6490240.

[13] M. C. Paredes Paredes, M. J. Fernández-Getino García, Comparison of architectures for PAPR reduction in OFDM combining pilot symbols with constellation extension, in: EUROCON, 2013 IEEE, 2013, pp. 391–398. doi:10.1109/EUROCON.2013.6625013.

[14] M. J. Fernández-Getino García, O. Edfors, J. M. Páez-Borrallo, Peak power reduction for OFDM systems with orthogonal pilot sequences, IEEE Transactions on Wireless Communications 5 (1) (2006) 47–51. doi:10.1109/TWC.2006.1576525.

[15] M. C. Paredes Paredes, M. J. Fernández-Getino García, Performance evaluation of ops-sap papr reduction technique in ofdm systems in a wireless vehicular context, in: Proceedings of the 12th ACM Symposium on Performance Evaluation of Wireless Ad Hoc, Sensor, & Ubiquitous Networks, ACM, 2015, pp. 49–54.

[16] A. M. Abdelgader, W. Lenan, The Physical Layer of the IEEE 802.11p WAVE Communication Standard: The Specifications and Challenges, in: Proceedings of the World Congress on Engineering and Computer Science, Vol. 2, 2014.

[17] J. A. Fernandez, K. Borries, L. Cheng, B. Vijaya Kumar, D. D. Stancil, F. Bai, Performance of the 802.11 p physical layer in vehicle-to-vehicle environments, Vehicular Technology, IEEE Transactions on 61 (1) (2012) 3–14.

[18] J. Tellado, Multicarrier modulation with low PAR: applications to DSL and wireless, Kluwer Academic Publishers, 2002.

[19] H. Ochiai, H. Imai, On the distribution of the peak-to-average power ratio in OFDM signals, IEEE Transactions on Communications 49 (2) (2001) 282–289. doi:10.1109/26.905885.

[20] K. Hong, D. Xing, V. Rai, J. Kenney, Characterization of DSRC performance as a function of transmit power, in: Proceedings of the sixth ACM international workshop on Vehicular Internetworking, ACM, 2009, pp. 63–68.

[21] M. Honkanen, S.-G. Haggman, New aspects on nonlinear power amplifier modeling in radio communication system simulations, in: The 8th IEEE International Symposium on Personal, Indoor and Mobile Radio Communications (PIMRC), Vol. 3, 1997, pp. 844–848. doi:10.1109/PIMRC.1997.627005.

[22] F. Abrate, A. Vesco, R. Scopigno, An analytical packet error rate model for WAVE receivers, in: IEEE Vehicular Technology Conference (VTC Fall), 2011, IEEE, 2011, pp. 1–5.

Martha Cecilia Paredes Paredes received her Eng. degree from Escuela Politécnica Nacional (EPN), Quito, Ecuador in 2008, the M.Sc. and Ph.D of Multimedia and Communications from Carlos III University of Madrid, Spain in 2010 and 2014, respectively. Also, from 2010 to 2011 she worked as an Assistant Lecturer at Universidad de las Americas (UDLA), Quito - Ecuador. She is currently an Assistant Professor at Departamento de Electrónica, Telecomunicaciones y Redes de Información (DETRI), EPN, Quito, Ecuador. Her research interests include multicarrier communications, OFDM transmissions, 5G networks and signal processing for wireless communications.

M. Julia Fernández-Getino García received the M. Eng. and Ph.D. degrees in telecommunication engineering from the Polytechnic University of Madrid, Spain, in 1996 and 2001, respectively. She is currently with the Department of Signal Theory and Communications, Carlos III University of Madrid, Spain, as an Associate Professor. From 1996 to 2001, she held a research position with the Department of Signals, Systems and Radiocommunications, Polytechnic University of Madrid. She visited Bell Laboratories, Murray Hill, NJ, USA, in 1998; visited Lund University, Sweden, during two periods in 1999 and 2000; visited Politecnico di Torino, Italy, in 2003 and 2004; and visited Aveiro University, Portugal, in 2009 and 2010. Her research interests include multicarrier communications, coding and signal processing for wireless systems. She received the best "Master Thesis" and "Ph.D. Thesis" awards from the Professional Association of Telecommunication Engineers of Spain in 1998 and 2003, respectively; the "Student Paper Award" at the IEEE International Symposium on Personal, Indoor and Mobile Radio Communications (PIMRC) in 1999; the "Certificate of Appreciation" at the IEEE Vehicular Technology Conference (VTC) in 2000; the "Ph.D. Extraordinary Award" from the Polytechnic University of Madrid in 2004; the "Juan de la Cierva National Award" from AENA Foundation in 2004; and the "Excellence Award" from Carlos III University of Madrid in 2012 for her research career.